Assessment of CUPID1.7 Code with PSBT Subchannel Test

Y. J. Cho, H. Y. Yoon
Korea Atomic Energy Research Institute, 111 Daedeok-daero, 989 Beon-gil, Yuseong-gu, Daejeon
Corresponding author: yjcho@kaeri.re.kr

1. Introduction

KAERI has developed CUPID1.7 (Component Unstructured Program for Interfacial Dynamics 1.7) code for a high-resolution analysis of two-phase flows in nuclear components [1]. Since CUPID code has been developed, various verification and validation (V&V) problems were solved to confirm not only the numerical stability, robustness and accuracy, but also the adequacy of physical models in CUPID code. Recently, as boiling models was improved, an additional V&V problem was required to validate newly implemented models. A PWR Sub-channel and Bundle Test (PSBT) is the international benchmark problem which is proper to validate the boiling models under the conditions of high pressure and high heat flux. In this paper, a single sub-channel test in PSBT was simulated. By using the calculation results, qualitative analysis was performed as well as quantitative comparison with the test data were performed.

2. PSBT Subchannel Test

2.1 Test Geometry

The PSBT subchannel test simulates one of the subchannel in a PWR fuel assembly as shown in Fig. 1. The total height of the channel is 1.555 m and the area averaged void fraction is measured at 1.400 m of height from the bottom. The width of the channel is 0.0126 m corresponding to the pitch distance between two fuel rods in a PWR [2].

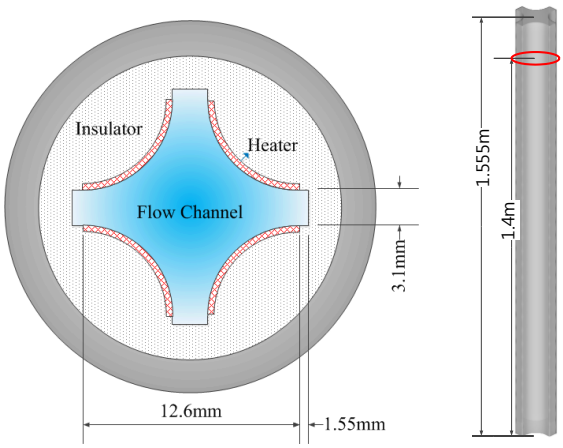

Fig. 1. Geometry of PSBT single subchannel test

2.2. Test Condition

The PSBT subchannel tests were performed with 4 varying control parameters: the pressure, mass flux, induced heater power, and inlet fluid temperature. The test result was given as the area averaged void fraction measured at 1.4 m height.

Among the 43 test datasets in the PSBT subchannel test opened as an international benchmark problem, 5 test cases were analyzed with CUPID1.7. As shown in Table 1, the cases were selected with considering the test ranges of pressure, temperature, and inlet condition so that the capability of CUPID1.7 to simulate the boiling phenomena with various ranges of void fraction was validated.

Table. 1. Calculation matrix

Run. No.	Pressure (MPa)	Mass flux (10^6kg/m^2 hr)	Power (kW)	Inlet Temp. (^{o}C)	Void faction
1.2211	14.72	10.9	90.0	295.4	0.038
1.3223	12.25	11.1	60.1	319.7	0.546
1.4326	9.82	5.0	60.1	268.8	0.531
1.5223	7.41	5.0	49.9	263.8	0.647
1.6222	4.90	5.0	49.9	204.2	0.306

3. Boiling and Non-drag Models in CUPID1.7

3.1 Boiling Heat Transfer Models

CUPID1.7 uses a wall heat partitioning model to simulate the sub-cooled boiling near walls. The heat flux from a wall is distributed to mainly three components: the surface quenching (q_q), the evaporation (q_e), and the single phase convection (q_{wlc} and q_{wg}) [3]. Eq. (1) shows the heat flux conservation, which turns into a non-linear equation for the wall temperature. In Eq. (1), α and q mean the volume fraction and heat flux. Subscripts *l*, *g*, *cm*, *bc*, *wlc*, *wg*, and *sat* are the liquid, gas, churn-mist transition, bubble-churn transition, wall-to-liquid continuous phase, wall-to-gas, and saturation, respectively.

$$q_{wall} = \frac{\alpha_{g,cm} - \alpha_g}{\alpha_{g,cm} - \alpha_{g,bc}} \left(q_q + q_e + q_{wlc} \right) + \frac{\alpha_g - \alpha_{g,bc}}{\alpha_{g,cm} - \alpha_{g,bc}} q_{wg} \quad (1)$$

The wall vapor generation rate (Γ) is calculated by Eq. (2) and Eq. (3) where *h*, *N*, *f*, and D_d are the enthalpy, nucleate site density, departure frequency, and departure bubble diameter, respectively.

$$\Gamma_{wall} = \frac{q_e}{\left(h_{g,sat} - h_l \right)} \quad (2)$$

$$q_e = Nf\left(\frac{\pi}{6}D_d^3\right)\rho_g h_{lg} \quad (3)$$

3.2 Non-drag Force Models

The void distribution in the cross-section is strongly affected by non-drag forces such as the wall lubrication force, bubble lift force, and turbulence dispersion force. In CUPID1.7

CUPID1.7 uses the wall lubrication force model suggested by Antal [4] as shown in Eq. (4).

$$\mathbf{M}_l^{WL} = -\frac{\alpha_g \rho_l C_{WL}\left|\vec{U}_g - \vec{U}_l\right|^2}{D_b}\max\left(0, C_1 + C_2\frac{D_b}{y_{wall}}\right)\vec{n}_{wall} \quad (4)$$

where D_b, U_g, U_l, and y_{wall} are the bubble diameter, gas velocity, liquid velocity, and the distance from the wall, respectively. C1 and C2 are additional constants, which are defined as -0.01 and 0.05, respectively.

The lift force is modeled as shown in Eq. (5).

$$\mathbf{M}_l^{lift} = \alpha_g \rho_l C_L\left(\vec{U}_g - \vec{U}_l\right)\otimes\left(\vec{\nabla}\otimes\vec{U}_l\right) \quad (5)$$

The turbulence dispersion force is predicted by Lahey model [5] as shown in Eq. (6).

$$\mathbf{M}_l^{TD} = -C_{TD}\rho_l k_l \nabla\alpha_l \quad (6)$$

where k is the turbulent kinetic energy.

In Eqs. (4) – (6), the constant values were applied for the coefficients of the wall lubrication force (C_{WL}), lift force(C_L), and turbulence dispersion force (C_{TD}).

4. CUPID1.7 Calculation

4.1 Grid Generation and Grid Sensitivity Calculations

With distribution of CUPID1.7, in-house grid generation program named CUPID-POP (CUPID-Polygon Based Prism) was developed. The CUPID-POP used Delaunay triangle and Voronoi polygon to assure an orthogonality of grids in a plane.

In the PSBT subchannel test, the gradient of the physical variables in the cross-section such as the velocity, temperature, and void fraction are much larger than those in the flow direction because the width of the flow channel is small and the high heat flux was induced into the side wall. Therefore, the grids smaller than 1.0 mm were used in the cross-section while the grid sizes with order of 10 mm were used in the z-direction.

To investigate the effect of grid size, a grid sensitivity calculation was performed with Run No. 1.2211. The numbers of grids in the cross-section were varied by 115, 330, 727, 1492, and 2876 while the number of grids in the z-direction was maintained as a constant. Fig. 2 shows the generated grid which has 727 grids in the cross-section. The heaters were not simulated in the CUPID1.7 calculation. Instead, the heat flux boundary condition was applied to the wall where the interface between the heaters and the flow channel is defined

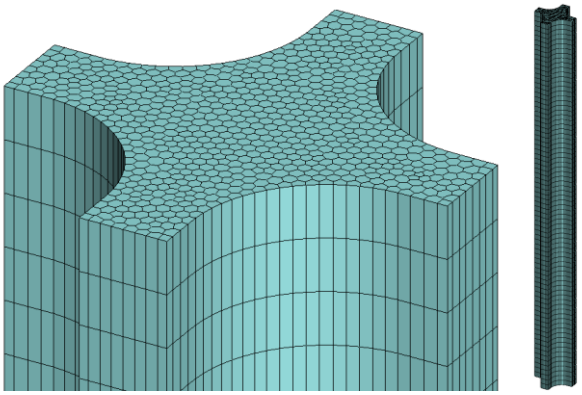

Fig. 2. Computational grid

Fig. 3 shows the area averaged void fraction with varying the number of grids in the cross-section. As the number of grids increases, the predicted void fraction also increases. However, the increasing rate is much higher when the coarse grids were used than the relatively fine grids were used. Therefore, the case of 727 grids in the cross-section was selected because the increasing rate of the predicted void fraction according to the number of grids was started to significantly decrease after that point.

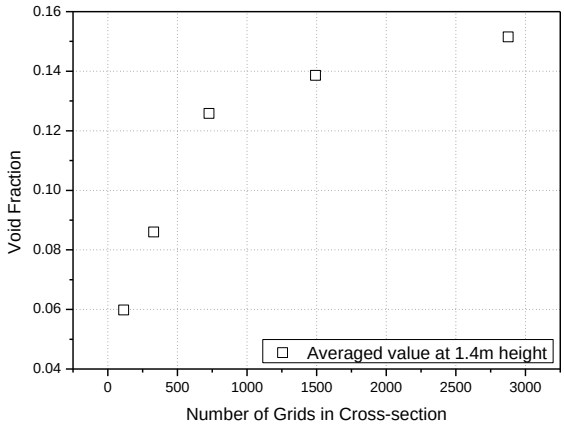

Fig. 3. Result of grid sensitivity test

The effect of grid size is not completely eliminated even though relatively fine grid size is used. The reason is assumed that the volumetric heat source increases when the first cell from the side wall is fine because the boundary condition of heat flux at the side wall is applied. High volumetric heat source causes an increase of fluid temperature as well as a vapor generation.

4.2 Sensitivity Calculations for coefficients in Non-drag Force Models

Although many researchers has developed the correlations for C_{WL}, C_L, and C_{TD} or suggested C_{WL}, C_L, and C_{TD} as constant values, it is difficult to find the correlation or the constant which shows good prediction

under the conditions of wide ranges of pressure, temperature, heat flux, and void fraction.

As preliminary work for the implementation of models for C_{WL}, C_L, and C_{TD}, the sensitivity calculations were performed with varying three coefficients with different constant values. Because there are well-known constant values for C_{WL}, C_L, and C_{TD} that are frequently used in commercial CFD codes, the sensitivity calculations were performed based on those values. Run. No. 1.2211 was selected for the calculation.

Fig. 4, Fig. 5, and Fig. 6 show the results of sensitivity calculations with varying C_{WL}, C_L, and C_{TD}, respectively. The figures show the distribution of void fraction from the channel center to the heated wall. As shown in Fig. 4, the coefficient of wall lubrication force affects the void fraction near wall. As we expect, the void fraction near wall decreases as the C_{WL} increases. However, the area-averaged void fraction at 1.4 m height was not changed significantly.

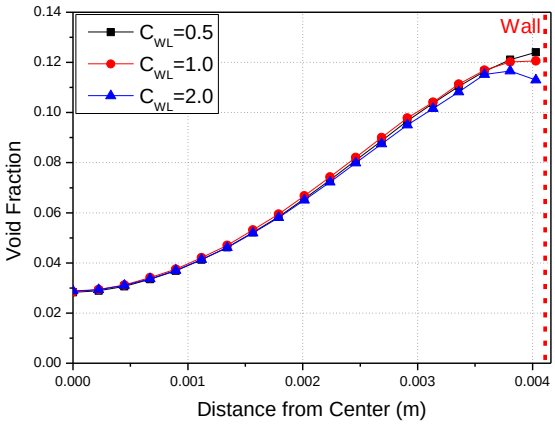

Fig. 4. Void fraction profile with varying C_{WL}

When C_{TD} increases, the distribution of void fraction becomes flat so that the peak value of the void fraction near wall decreases. The change of distribution also affects the area-averaged void fraction. As C_{TD} increases from 0.05 to 0.4, the area-averaged void fraction decreases from 0.1223 to 0.0956.

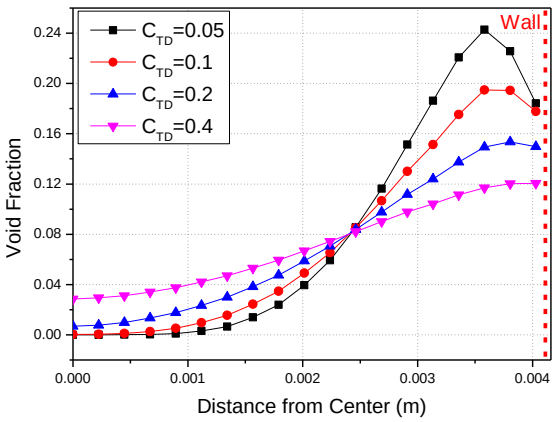

Fig. 5. Void fraction profile with varying C_{TD}

C_L also affects the distribution of void fraction as shown in Fig. 6. It seems that the peak of void fraction become closer from the wall as C_L increases. However, it does not change the area-averaged void fraction significantly.

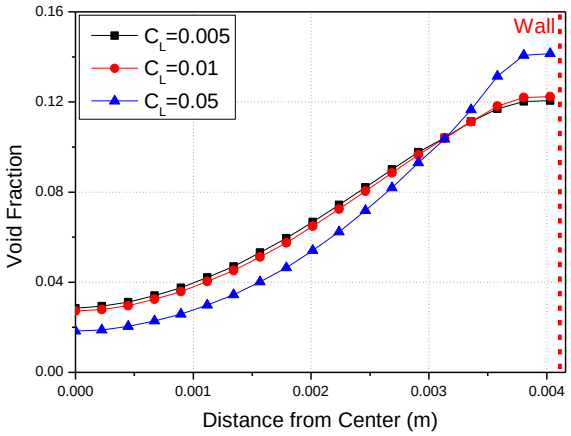

Fig. 6. Void fraction profile with varying C_L

4.3 Comparison Results

The calculation results for 5 test cases summarized in Table 1 were compared in Table 2. CUPID1.7 generally over-predicted the area-averaged void fraction except the Run. No. 1.3223. In particular, CUPID1.7 highly overestimated the case of Run. No. 1.2211 which has the lowest void fraction among 43 sub-channel tests. This kind of overestimation in the test case with very low void fraction was also observed other researches using a commercial CFD code [6, 7]. Except the Run. No. 1.2211, CUPID 1.7 generally predicts well the area-averaged void fraction within the maximum discrepancy of 31.6 %.

Table 2. Comparison results

Run. No.	Void faction (Exp.)	Void faction (CUPID)
1.2211	0.038	0.0956
1.3223	0.546	0.5064
1.4326	0.531	0.6226
1.5223	0.647	0.7041
1.6222	0.306	0.4027

Since the vapor generation and distribution is governed by the wall heat partitioning model and interfacial heat transfer model, it is necessary to determine proper models applicable to the test conditions such as the system pressure, temperature, flow velocity, etc. In particular, very sensitive model is required for the low void fraction condition.

Although PSBT sub-channel test did not provide any information on the distributions of void fraction and

velocity at the cross-section according to the flow length, the calculation results for the distribution was evaluated for the qualitative assessment.

Fig. 6 shows the simulation results for the distributions of void fraction and liquid velocity along the test channel in Run. No. 1.2211. The aspect ratio of the channel is reduced to 1/50 in the figure for visibility. Three planes sliced in the z-axis are generated at 0.9m, 1.4m, and 1.55m heights from the bottom of the channel.

Sub-cooled boiling begins to occur near the heated wall from around 0.9m height of the test channel and, then, the void fraction increases along the test channel as shown in the left figure. The void fraction is higher at the heated wall than that at the center of the channel. This result implies that a model is required to move the peak of void fraction from the wall to the center. This model can be a bubble coalescence model or a wall lubrication model.

As shown in the right figure, The liquid velocity shows the core-peaking shape and reaches fully developed condition near the exit of the channel.

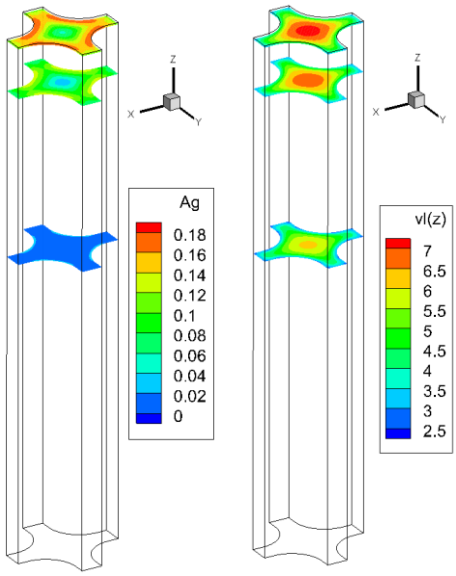

Fig. 6. Distributions of void fraction and liquid velocity in Run. No. 1.2211

5. Conclusions

The PSBT subchannel test was simulated in order to assess the wall heat partitioning model and non-drag force models in CUPID1.7. The simulation results showed that CUPID1.7 properly predicts the sub-cooled boiling near a wall and behavior of the void fraction distribution. However, CUPID1.7 overestimated the area-averaged void fraction compared to the test data, especially for the case with very low void fraction. This result indicates that an improvement and validation of the boiling model or interfacial area transport model are required. In addition, the turbulence model should be validated simultaneously with the boiling model since the turbulence behavior affects the temperature and velocity profile near a wall.

ACKNOWLEDGMENTS

This work was supported by National Research Foundation of Korea (NRF) grant funded by the Korea government (MSIP).

REFERENCES

[1] J. J. Jeong, et al., The CUPID code development and assessment strategy, Nuclear Engineering and Technology, Vol. 42, No. 6, 2010.
[2] A. Rubin, at al., OECD/NRC benchmark based on CUPEC PWR subchannel and bundle tests (PSBT) Volume I: Experimental database and final problem specifications, US NRC, NEA/NSC/DOC(2010)1, 2010.
[3] H. K. Cho, et al., Recent improvements to the multi-dimensional semi-implicit two-phase flow solver, CUPID, Proceedings of the 17th International Conference on Nuclear Engineering (ICONE17), July 12-16, Brussels, Belgium, 2009.
[4] S. P. Antal, R. T. Lahey, J. E. Flaherty, Analysis of phase distribution in fully developed laminar bubble two-phase flow, International Journal of Multiphase Flow, Vol. 7, pp. 635-652, 1991.
[5] R. T. Lahey, M. Lopez de Bertodano, O. C. Jones, Phase distribution in complex geometry conduits, Nuclear Engineering and Design, Vol. 141, pp. 177-201, 1993.
[6] E. Krepper, R. Rzehak, CFD analysis of a void distribution benchmark of the NUPEC PSBT tests: Model calibration and influence of turbulence modeling, Science and Technology of Nuclear Installations, Vol. 2012, 2012.
[7] W. K. In, C. H. Shin, C. Y. Lee, CDF simulation of subcooled boiling flow in nuclear fuel bundle, Seventh International Conference on Computational Fluid Dynamics (ICCFD7), Hawaii, July 9-13, 2012.